Use of Numerical Modeling to Assess Instrumented Root Piles Subjected to Axial Compression

Jean Rodrigo Garcia
PhD Student, School of Civil Engineering, State University of Campinas
Campinas, São Paulo, Brazil
e-mail: eng.garcia@gmail.com

Paulo José Rocha de Albuquerque
School of Civil Engineering, State University of Campinas
Campinas, São Paulo, Brazil
pjra@fec.unicamp.br

ABSTRACT

An analysis was performed on the behavior of a root pile (ϕ = 0.31 m and L = 23m) instrumented at depth and then subjected to slow loading tests (SML). This analysis was conducted in Campinas, São Paulo. The results were compared to those obtained by strain gage instrumentation both via the analytical method and also via three-dimensional numerical modeling by the finite element method, which allows a simulation of the elastic-plastic behavior of the soil. Cambefort ratios were also employed to analyze portions of frictional and lateral tip resistance. The local subsoil is composed of residual diabase soil. The geotechnical parameters of soil resistance were determined by means of empirical and semi-empirical correlations via mechanical CPT test values (Begeman cone). The values for the number of blow (N) obtained from the SPT test confirmed the soil characteristics. The load test was taken up to a maximum load of 2000 kN with total displacement of 29.76 mm and 2.31 mm for half the maximum load (1000 kN). The tipo contribution it was approximately 12% for the maximum load of the test.

KEYWORDS: Root pile, embedded in soil, instrumented, three-dimensional numerical analysis.

INTRODUCTION

The major challenge facing foundation engineering is to understand the behavior of foundations, particularly with regard to load-bearing capacity and load transfer. The technical community uses analytical tools as common practice to determine the forces that act on deep foundations. At times, instrumented load tests are used in order to understand the various phenomena as well. Numerical tools based on the finite element method (FEM) or boundary element method (BEM) are current practice, but the quality of the results is linked to the quality of the input parameters. The aim of the present study is to evaluate the load-bearing capacity of root piles by performing a load test on a root pile using instruments at depth and an FEM-based numerical tool. The results obtained with these two distinct tools will be assessed.

The ultimate load-bearing capacity (R) of one separate pile subjected to axial compressive forces and embedded in cohesive soil can be evaluated using expressions 1, 2 and 3 (below) derived from the Theory of Plasticity, by taking into account the sum of the parts resulting from tip resistance (R_p) and lateral resistance (R_L):

$$R = R_p + R_L - W \tag{1}$$

$$R_p = q_b \cdot A_b = (s_u \cdot N_c) \cdot A_b \tag{2}$$

$$R_L = q_s \cdot A_s = (\alpha \cdot s_{u,avg}) \cdot A_s \tag{3}$$

where: A_b = the cross-sectional area at the tip of the pile; A_s = the lateral area of the pile; $s_{u,avg}$ = mean undrained soil cohesion along the pile shaft; s_u = soil cohesion at the tip of the pile; N_c = load-bearing capacity factor; α = adhesion factor; W = weight of the pile itself; q_s = unit lateral friction (≤380kPa).

The lateral pile resistance given by equation 3 produces several uncertainties, as the parameters are heavily influenced by the construction procedure and may vary significantly along the length of the pile shaft (Fioravante et al., 1995). As a consequence, average cohesion is determined layer by layer, corresponding to the respective unit lateral area of the pile shaft. Thus the computation of the adhesion factor (α) may be performed per the proposed ratio (O'Neill & Reese, 1999), as follows:

$$\alpha = \begin{cases} 0.55 & \text{for } c_u / p_a \le 1.5 \\ 0.55 - 0.1 \cdot \left(\dfrac{c_u}{p_a} - 1.5 \right) & \text{for } 1.5 < c_u / p_a \le 2.5 \end{cases}$$

where: p_a = atmospheric pressure: 101 kPa.

As to the portion relating to tip resistance (R_p), two aspects must be taken into consideration: resistance increases in a linear fashion with depth up to a specific limit (Meyerhof, 1976, Vésic, 1964 and Vésic, 1970) and resistance tends towards saturation with the increase in confinement strain (Fleming et al., 2009). For longer piles, the appropriate value for N_c is 9 (Skempton, 1951), although it is permitted to consider the depth that the pile tip penetrates into the rigid layer (beneath the soft soil) for just a few meters in depth. Thus linear interpolation may be carried out between a value of N_c = 6, for the case of a pile tip only reaching the rigid layer, and N_c = 9, where the pile tip penetrates three or more diameters into the rigid layer.

$$N_c = \begin{cases} 9.0 & \text{for } h_{penet.} \ge 3B \\ 6 + \dfrac{h_{penet.}}{B} & \text{otherwise} \end{cases}$$

To understand more deeply the model of load transfer in piles, Cambefort's Laws are employed (Cambefort, 1964), since their ratios mathematically represent the elementary understanding of soil-pile interaction. These laws set out ratios of a rigid-elastic-plastic nature, both for lateral friction and for the reaction of pile tips.

To assess Cambefort ratios, the present study used instrumentation to capture extremely precise load distribution data along predetermined sections of the pile. Thus it was found that there is a significant need to carry out instrumented load tests on piles in order to understand more about the behavior of deep foundations (Albuquerque, 2001).

The estimation of geotechnical parameters from formulations based on field trials enables us to ascertain with greater precision the behavior of the load-settlement curve obtained through the numerical model (Garcia et al., 2013). Therefore in this study, the estimate of resistance parameters of surface soil layers was obtained from empirical and semi-empirical correlations to get estimated values for cohesion, angle of friction and modulus of elasticity at depth, as shown in equations 4, 5, 6 and 7.

To compute the modulus of elasticity of soil layers characterized by clayey behavior, the equation defined for Frankfurt clay is used (Reul, 2000):

$$\mathrm{E} = 45 + \left(\tanh\left(\frac{\mathrm{z}-30}{15}\right) + 1\right) \cdot 0{,}7 \cdot \mathrm{z} \ \text{(in kPa)} \tag{4}$$

The ratio between modulus of deformability, E, and cone tip resistance (q_c - σ_{vo}) for different soils is as follows (Kulhawy & Mayne, 1990):

$$E = 8{,}25 \cdot (q_c - \sigma_{v0}) \text{ (in kPa)} \tag{5}$$

The angle of friction (ϕ) values were computed using correlations developed for sandy soil (Kulhawy & Mayne, 1990), as shown below:

$$\phi = tan^{-1} \cdot \left(0{,}1 + 0{,}381 \cdot \log\left(\frac{q_c}{\sigma_{v0}}\right)\right) \tag{6}$$

where:
q_c - CPT cone resistance measurements;
σ_{v0} - effective vertical tension at depth.

For an estimate of undrained resistance of clayey soils based on the piezocone test, equation 7 may be used with N_K assuming values ranging from 15 to 20 (Lunne et al., 1997).

$$\mathrm{s_u} = \frac{\mathrm{q_c} - \sigma_{v0}}{N_K} \quad \text{(kPa) with } \mathrm{N_K} = 20 \tag{7}$$

where: N_K - parameter of reduction in cone tip resistance to get undrained shear resistance.

$$\mathrm{c_u} = S_u \cdot 0{,}5 \tag{8}$$

where: c – cohesion.

ESTIMATES OF GEOTECHNICAL PARAMETERS

Figure 1 shows the result of the SPT test. However, to estimate the geotechnical parameters of the local subsoil, CPT-type field trials were performed at depth, as shown in figure 2.
Figure 2 shows the mean values of q_c, f_s and R_f, which are used as the base parameters to get the soil mechanical characteristics required for numerical analyses (figures 3, 4 and 5), along with N_{SPT} values to estimate the values of c_u.(equation 8 and figure 6).

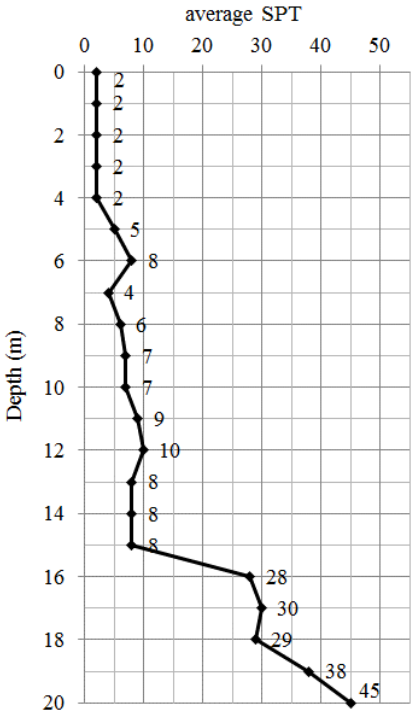

Figure 1: SPT sounding profile

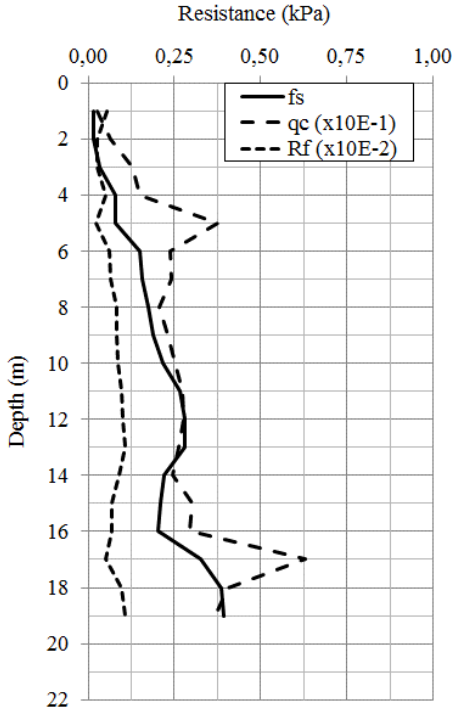

Figure 2: CPT test values

Figure 1 shows a sharp increase in N_{SPT} values starting from a depth of 15 m, as well as the limitation of these soundings by percussion at a depth of 20 m.

Based on the results of these tests, it was possible to ascertain that the subsoil is composed of diabase soil with a surface layer approximately 6.5 m thick composed of highly porous silt and sandy clay, followed by a layer of clayey-sandy silt down to a depth of 19 m. The water table is found at 17 m. Using the Robertson & Campanella chart to classify this soil, a friction ratio parameter (R_f) is obtained which is concentrated mostly in zone 7 (silty sand to sandy silt), in contrast to the behavior obtained using the visual and tactile classification (Fontaine, 2004).

Table 1 displays the values of geotechnical parameters of the different layers that make up the subsoil, as used in the numerical analyses.

Table 1: Parameters for numerical modeling
γ - Specific weight (kN/m³); c - cohesion (kN/m²); φ - angle of friction (°);
ν - Poisson Coefficient; Ei - Modulus of elasticity (MPa)

Soil layer	γ	c	φ	ν	Ei
0 - 6m	14.0	24.5	33.1	0.3	11.8
7 - 14m	14.8	77.7	29.3	0.4	17.9
15 - 23m	16.5	182.9	27.3	0.4	28.6
24 - 30m	18.0	243.0	25.1	0.4	32.5

It can be seen from figures 1, 2, 3, 5 and 6 that the soil resistance parameters increase with depth, except for the angle of friction values, which decrease with depth, tending towards stabilization (figure 4).

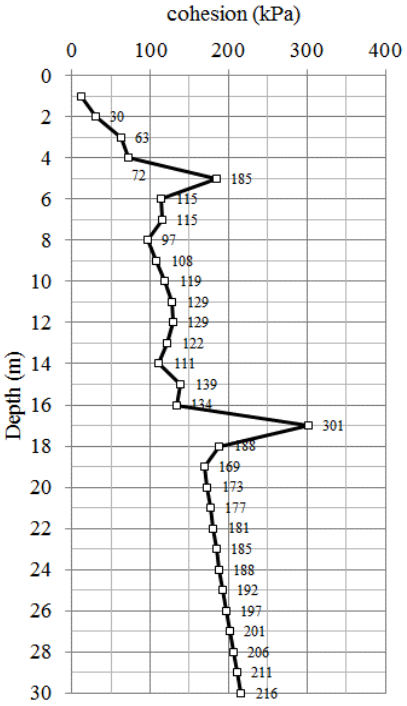

Figure 3: Variation in cohesion at depth.

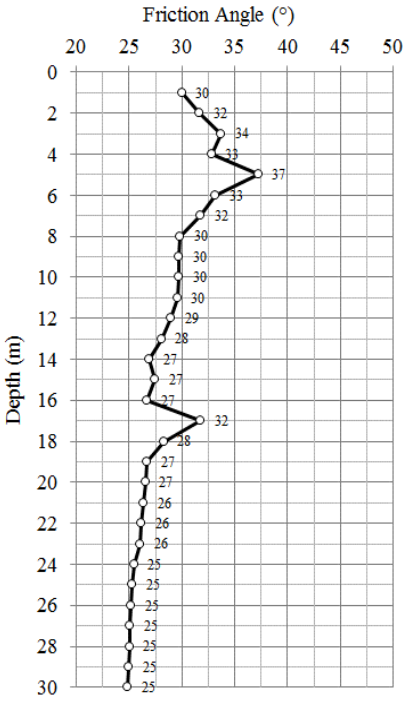

Figure 4: Variation in angle of friction at depth.

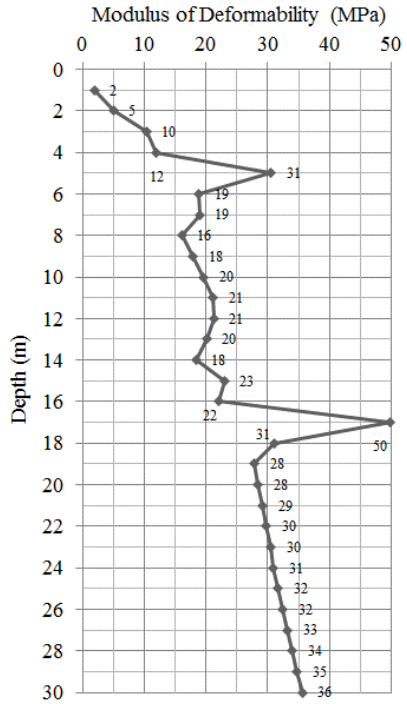

Figure 5: Variation in modulus of deformability at depth, for sandy soil.

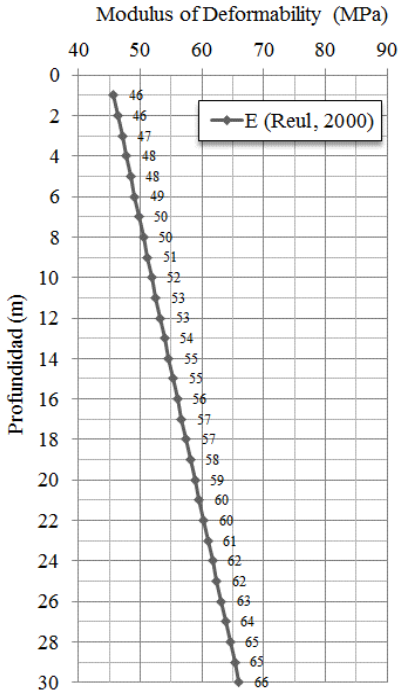

Figure 6: Variation in modulus of deformability at depth for clayey soil.

ROOT PILE AND INSTRUMENTATION

The nominal diameter of the pile under study is 310 mm and the length is 23 m. It was tested via axial compression. The instruments used were of the type of instrumented bars with strain-gages installed at the following depths: 0.5 m (N1* - reference), 5 m (N2 - unserviceable), 11.7 m (N3), 18 m (N4) and 22.7 m (N5), distributed along the pile shaft (Garcia, 2006). The use of instrumentation at various levels made it possible to check and quantify load values at each level as well as mobilizations caused by skin friction and tip load for each load increment while the load test was being conducted.

The graph in figure 7 shows the deformation obtained in the reference section for each load level. The instrument placed at the -5m quota was disregarded because it produced inconsistent results.

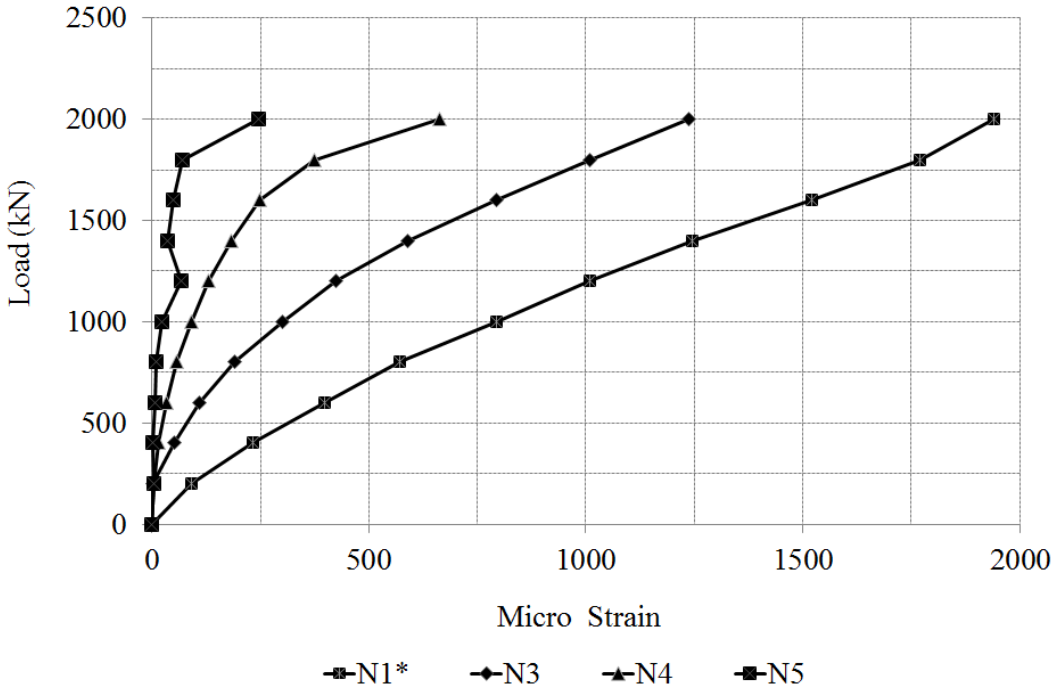

Figure 7: Load distribution vs deformation (Garcia, 2006).

Figure 7 demonstrates that the instrumentation worked perfectly, except for level 2 (5m), which did not work. Note that for the last load increment at the top, the tip displayed greater deformation, indicating greater mobilization of the tip. The pile's modulus of elasticity of 30 GPa demonstrates that it is close to the values stated in the literature.

LOAD TESTS

A static, slow load test (SML) was performed follow the Brazilian Standards (NBR 13131/92); in other words, the loadings were carried out in identical, successive stages, no greater than 20% of the work load established for each pile tested. The aforementioned load test was performed in the Experimental Field at UNICAMP, a public university in the city of Campinas, in the state of São Paulo.

NUMERICAL MODELING

The modeling was performed from ¼ of the problem in question due to the symmetry along the pile axis, resulting in a rectangular block with a 10m x 10m section and variable depth in conformance with the length of the pile being analyzed, but at least 10m below the tip of the pile. These dimensions were assigned as a function of tests conducted to ensure that the contour conditions assigned to the problem extremities could be considered as non-displaceable or else as having very low displacement and consequently would not impact the result of the analyses. An elastic-plastic model was employed that varies according to the strains applied, following a non-linear behavior model. The mesh of finite elements was composed of triangular elements with quadratic interpolation, which were extruded at each meter of depth.

The properties attributed to the various soil layers followed the Mohr-Coulomb failure criterion, i.e., values of specific weight (γ), cohesion (c), angle of friction (ϕ), modulus of deformation (E) and Poisson coefficient (ν) were entered. For those materials with fragile behavior (Parabolic Model), such as injection concrete and mortar, the following values were assigned: compressive strength, tensile stress (R_t), specific weight, modulus of deformation and Poisson coefficient.

RESULTS

There follows the experimental results from a load test and the respective numerical analysis by three-dimensional finite elements.

Figure 8 displays the result of the load test obtained for the tested pile and a graph comparing the load test performed to the numerical simulation, in which it was found that the maximum test load (Q_{max}) was 2000 kN both for the load test and for the numerical analysis. This Figure demonstrates that the load-settlement curve obtained by means of numerical analysis is more depressed in terms of magnitude of the settlement versus the results observed via the load test experimental curve.

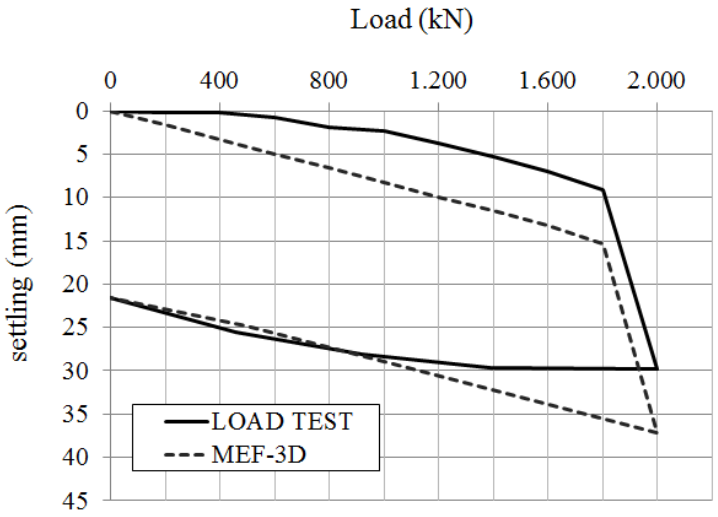

Figure 8: Load-settlement curve for the load test and numerical analysis of the pile.

The load-settlement curve in figure 8 indicates that, both experimentally and numerically, the final load stage at 2000 kN produces high levels of deformation, the settling values being equal to 30 mm and 3 7mm, respectively. It can be seen from these curves that the settling values for $½ \cdot Q_{máx}$ were 2 mm and 8 mm for the load test and numerical analysis, respectively.

Figures 9 and 10 show the respective load transfer behavior at depth obtained in both the load test and the numerical model for a maximum test load (2000 kN).

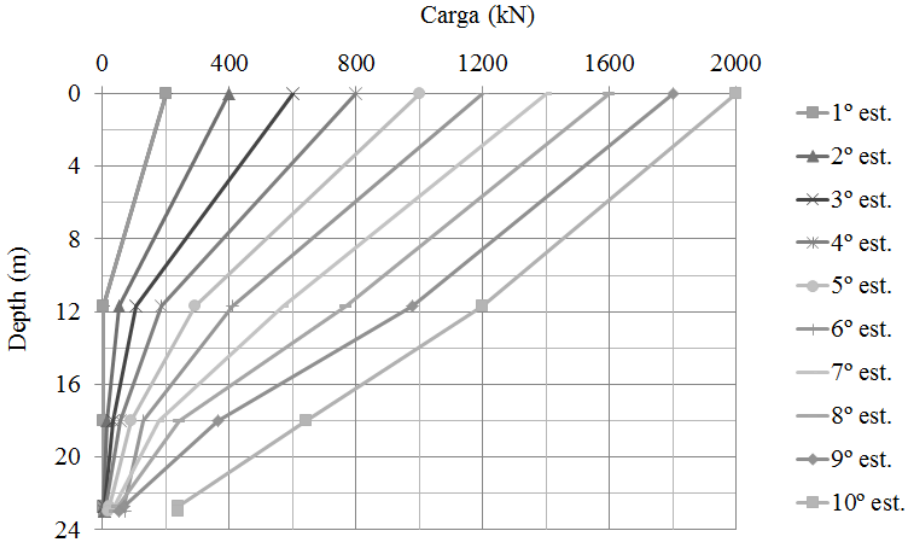

Figure 9: Load transfer of the root pile at depth (PC-2000kN).

Figure 9 indicates that the dissipation of the skin friction is uniform and continuous along the depth, with mean of approximately 78 kPa for the first section from 0 to 18m. Below this depth, there is an increase to 89 kPa in this skin friction and a tip portion of approximately 12% of the maximum test load (figure 9).

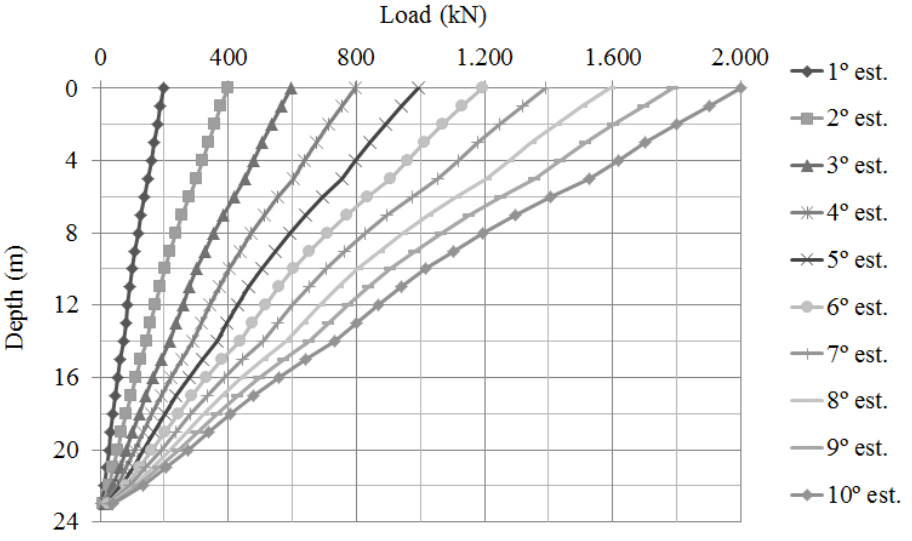

Figure 10: Load transfer of the root pile at depth (MEF-2000kN).

For the numerical simulation, it can be seen that the values are in the order of 91 kPa for the section from 0 to 18m and 17 kPa for the section from 18 to 23 m, with just 4% for the tip portion (figure 10).

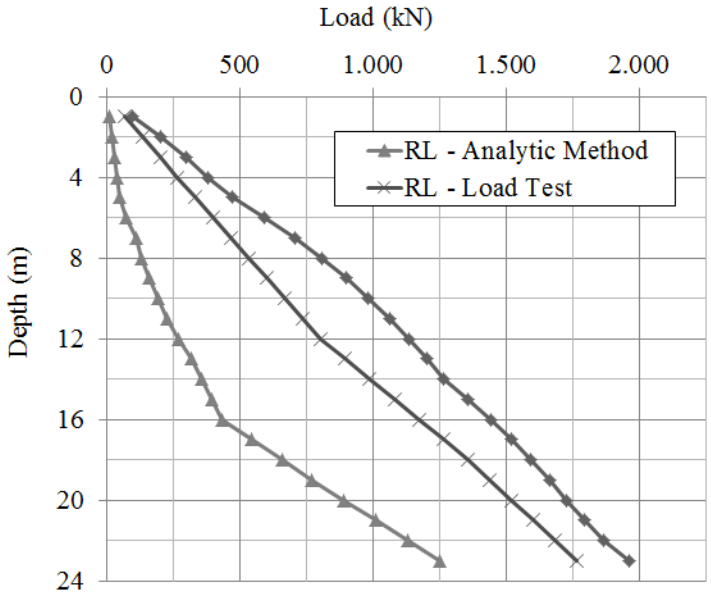

Figure 11: Distribution of lateral resistance via models of analysis for maximum load.

The cumulative gain in lateral resistance at depth can be seen in figure 11, which shows that the lateral resistance values obtained experimentally lie between the curve obtained using the numerical model and the analytical method.

According to the distributions through skin friction shown in figures 12 and 13, it can be seen that down to a depth of 18 m, 88% of the maximum load was absorbed by skin friction in the load test, whereas in the numerical analysis, this portion was in the order of 80 %. However, when the same condition was verified for $½Q_{max}$, it was found that, in the first section (0 to 18m), 98% of this load had been absorbed by skin friction in the load test, while in the numerical model, this remained at 80%.

The mean skin friction observed increased by 13% in comparison to the friction observed in the previous layer, as far as 18 m (figure 12). According to figure 13, however, it can be seen that, in the case of the numerical analysis, the opposite is true, i.e., there was a sharp fall in mean skin friction of approximately 82 % in comparison to the friction observed in the first layer.

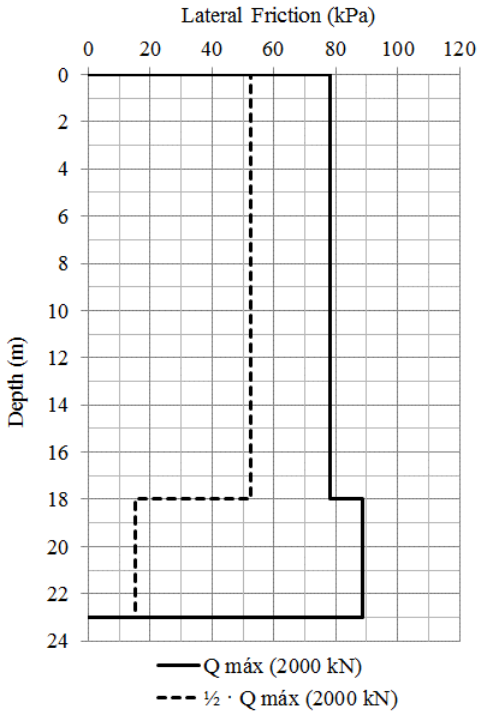

Figure 12: Distribution of friction obtained in the load test (load of 2000 kN).

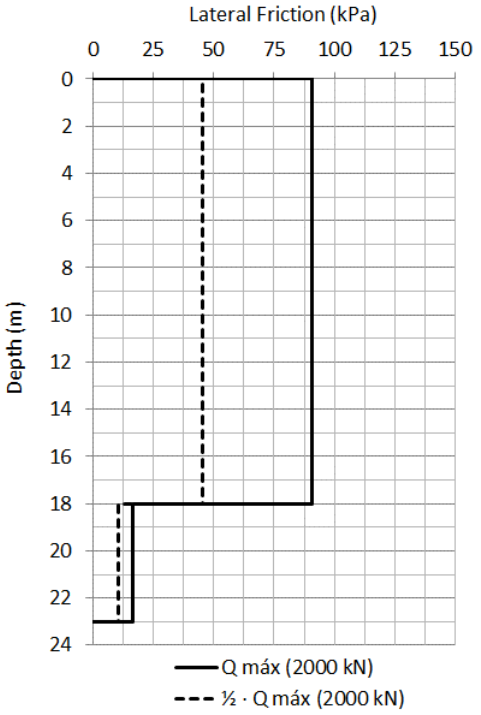

Figure 13: Distribution of friction obtained numerically for a load of 2000 kN.

Figures 14 and 15 show the Cambefort graphs of distribution of lateral friction and tip load as a function of displacements. Figure 14 shows that the value of tip resistance for the load test data rises with increased displacements, which is not the case with skin friction resistance, which remains constant beyond 8 mm and is practically nil for mean displacement above 25 mm (figure 15).

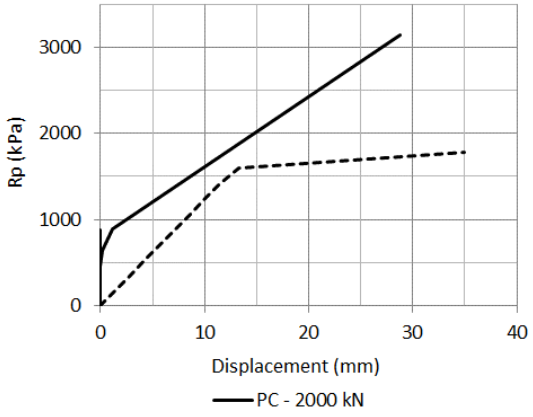

Figure 14: Mean lateral friction as a function of displacement for the load test and numerical analyses.

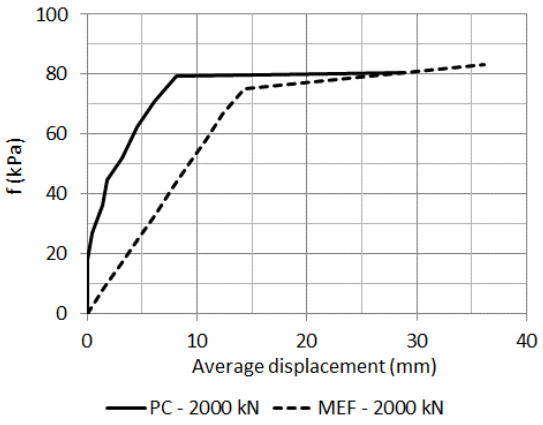

Figure 15: Average lateral friction as a function of displacements for the load test and numerical analyses.

Figure 14 (according to Cambefort's Law) indicates that the tip resistance begins its mobilization with displacements in the order of 0.8 mm starting from a strain at the tip in the order of 760 kPa. Note the upward trend of the tip resistance mobilization curve, which does not denote rupture but rather an increase in the value (Meyerhof, 1976, Vésic, 1964 and Vésic, 1970).

With regard to numerical modeling, note that as far as a displacement of 13 mm, an upward trend is shown with a low tendency towards a gain in resistance by the tip, thereby revealing probable stabilization close to a strain value of 1500 kPa.

The graphs in figure 15 demonstrate the value of maximum skin friction (saturation) and required displacements. In other words, in the case of the load test, the value of maximum skin friction was 80 kPa with displacement of 8 mm, whereas via the FEM it may be said that the value of maximum skin friction was 80 kPa with displacement of 14 mm, since a slight, though increasing, tendency towards gain in resistance with displacement can be noticed.

CONCLUSIONS

The estimation of geotechnical parameters using formulations based on in situ tests made it possible to calculate accurately the behavior of the load-settlement curve given by the numerical model. Therefore, the conclusion is that it is perfectly possible to use empirical and semi-empirical correlations to estimate soil parameters using in situ tests such as CPT.

The numerical model, using 3D finite elements, made it possible to acquire, with particular accuracy, the load distribution through skin friction at depth for values close to the rupture load.

However, for loads closer to 50% of the maximum test load, there is a tendency to underestimate the increase in load distribution for greater depths, even when there is a possibility of dissipation through skin friction due to the remaining lateral area.

The contribution of the tip was seen to be slightly higher in the load test at approximately 12%, against 4% in the numerical model for the same maximum test load of 2000 kN. The load test demonstrated that tip resistance increases for values close to the maximum load and shows greater mobilization of total resistance. This may be explained by the Cambefort ratios, which reveal depletion of resistance by skin friction and a tendency towards gain in resistance of the tip. This fact could not be verified in the treatment of numerical results by Cambefort ratios, where it is clearly possible to see that the tip tends to stabilize, even with a discrete upward shift in the tip resistance line.

The behavior of piles molded in situ may be obtained with greater accuracy through numerical analysis via 3D finite elements, as opposed to the analytical method evaluated.

The performance of instrumented load tests is recommended for piles molded in situ and injected under pressure to get a better understanding on the behavior of this type of foundation.

ACKNOWLEDGMENTS

The authors would like to thank the Coordination for the Improvement of Higher Education Personnel (CAPES) and the National Council for Scientific and Technological Development (CNPq).

REFERENCES

1. Albuquerque, P. J. R. (2001), Estacas escavadas, hélice contínua e ômega: Estudo do comportamento à compressão em solo residual de diabásio, através de provas de carga instrumentadas em profundidade. Tese de Doutorado, Escola Politécnica/USP, São Paulo. pp. 297.

2. Cambefort, H. (1964), Essai sur le comportement en terrain homogène des pieux isolés et des groupes de pieux. In: INSTITUT TECHNIQUE DU BATIMENT ET DES TRAVAUX PUBLICS, Paris. Annales… Paris, 1964.n. 204, pp. 1478-1517.

3. Fioravante, V., Ghionna, V.N., Jamiolkowski, M.B. and PEDRONI, S. (1995), Load carrying capacity of large diameter bored piles in sand and gravel. Proc. 10th Asian Regional Conference on ARSC-MFE, 2, pp. 3-15.

4. Fleming, K., Weltman, A., Randolph, M. and Elson, K. (2009), Piling Engineering, 3rd ed. Taylor & Francis, New York.

5. Fontaine, E. B. (2004), Utilização de ensaios geotécnicos especiais de campo, cone elétrico e pressiométrico, em solos do interior do estado de São Paulo. Tese de Doutorado, Feagri, Unicamp, Campinas, pp. 256.

6. Garcia, J. R. (2006) Estudo do comportamento carga vs recalque de estacas raiz carregadas à compressão. Dissertação de Mestrado, FEC, Unicamp, Campinas, pp. 189.

7. Garcia, J. R., Albuquerque, P. J. R., Perez, N. B. M. (2013), Análise experimental e numérica de estaca pré-moldada embutida em solo de diabásio. In: VII Seminário de Engenharia Geotécnica do Rio Grande do Sul, ANAIS DO VII SEMINÁRIO DE ENGENHARIA GEOTÉCNICA DO RIO GRANDE DO SUL. Santa Maria: ABMS/RS, 1, pp. 237-244.

8. Kulhawy, F. H. & Mayne, P. H. (1990), Manual on Estimating Soil Properties for Foundation Design. Electric Power Research Institute, EPRI.

9. Lunne, T., Robertson, P. K. e Powell, J. J. M. (1997), Cone Penetration Testing. Blackie Academic & Professional. London, United Kingdom.

10. Meyerhof, G. G. (1976), Bearing Capacity and Settlement of Pile Foundations, Journal of the Geotechnical Engineering Division, ASCE, Vol. 102, No. GT3, pp. 197-228.

11. O'Neill, W. M. and Reese, C. L. (1999), Drilled Shafts: Construction Procedures and Design Methods, FHWA-IF-pp. 99-025.

12. Reul, O. (2000), In-situ measurements and numerical studies on the bearing behaviour of piled rafts. Ph.D. study, Darmstadt University of Technology, Darmstadt, Germany.

13. Skempton, A.W. (1951), The Bearing Capacity of Clays, in Building Research Congress. London: ICE, pp. 180-189.

14. Vésic, A. S. (1964), Investigation of Bearing Capacity of Piles in Sand. Proc. No. Amer. Conf. on Deep Foundations, Mexico city, Vol. 1.

15. Vésic, A. S. (1970), Tests on Instrumented Piles - Ogeeche River Site, JSMFD, ASCE, Vol. 96, No SM2.